Mitochondrial Protection by Exogenous Otx2 in Mouse Retinal Neurons

Hyoung-Tai Kim, Soung jung Kim, Young-In Sohn, Sun-Sook Paik, Romain Caplette, Manuel Simonutti, Kyeong hwan Moon, Eun jung Lee, Kwang wook Min, Mi jeong Kim, et al.

Article

Cell Reports

Mitochondrial Protection by Exogenous Otx2 in Mouse Retinal Neurons

Graphical Abstract

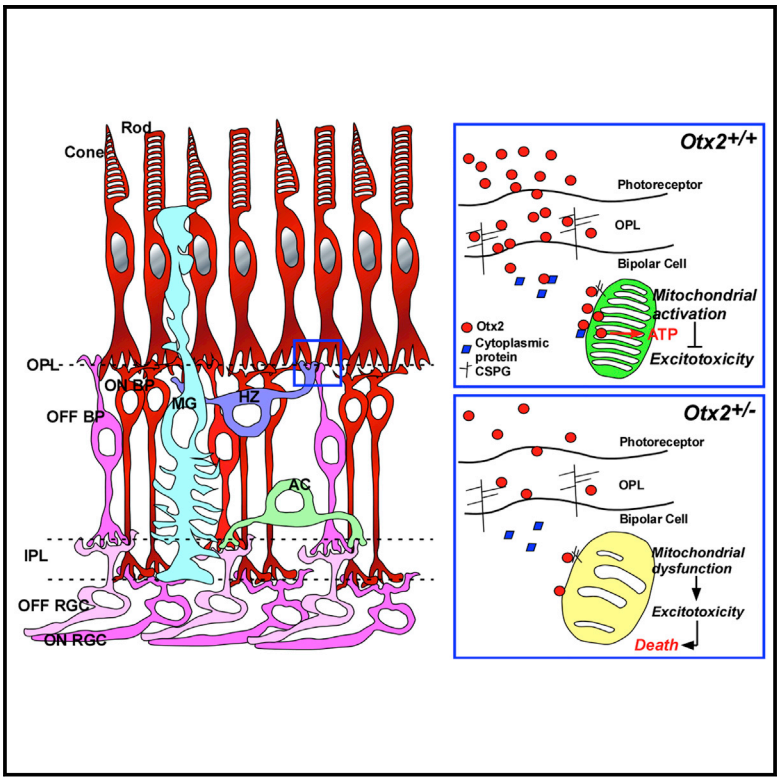

Highlights

- *Otx2* haplodeficiency results in retinal dystrophy in mice
- Otx2 proteins from photoreceptors are protective of retinal bipolar cells
- Exogenous Otx2 in bipolar cells is found into mitochondria and affects ATP synthesis
- Intraocular Otx2 injection restores retinal activity in *Otx2*$^{-/+}$ mice

Authors

Hyoung-Tai Kim, Soung Jung Kim, Young-In Sohn, ..., In-Beom Kim, Minho Shong, Jin Woo Kim

Correspondence

jinwookim@kaist.ac.kr

In Brief

Kim et al. propose a neuroprotective activity for exogenous OTX2 in mitochondria of retinal bipolar cells. The authors suggest that retinal dystrophy in *OTX2*-haplodeficient humans and mice is related to a decrease in the amount of OTX2 protein transferred to retinal bipolar cells.

Kim et al., 2015, Cell Reports *13*, 990–1002
November 3, 2015 ©2015 The Authors
http://dx.doi.org/10.1016/j.celrep.2015.09.075

OPEN ACCESS
CellPress

Cell Reports
Article

Mitochondrial Protection by Exogenous Otx2 in Mouse Retinal Neurons

Hyoung-Tai Kim,[1] Soung Jung Kim,[2] Young-In Sohn,[1] Sun-Sook Paik,[3] Romain Caplette,[4,5,6] Manuel Simonutti,[4,5,6] Kyeong Hwan Moon,[1] Eun Jung Lee,[1] Kwang Wook Min,[1] Mi Jeong Kim,[7] Dong-Gi Lee,[8] Antonio Simeone,[9,10] Thomas Lamonerie,[11] Takahisa Furukawa,[12,13] Jong-Soon Choi,[8] Hee-Seok Kweon,[7] Serge Picaud,[4,5,6] In-Beom Kim,[3] Minho Shong,[2] and Jin Woo Kim[1,*]

[1]Department of Biological Sciences, Korea Advanced Institute of Science and Technology (KAIST), Daejeon 305-701, South Korea
[2]Research Center for Endocrine and Metabolic Diseases, Chungnam National University School of Medicine, Daejeon 301-721, South Korea
[3]Department of Anatomy, College of Medicine, The Catholic University of Korea, Seoul 137-701, South Korea
[4]INSERM, U968, Paris 75012, France
[5]Sorbonne Universités, UPMC Univ Paris 06, UMR_S 968, Institut de la Vision, Paris 75012, France
[6]CNRS, UMR_7210, Paris 75012, France
[7]Nano-Bio Electron Microscopy Research Group, Korea Basic Science Institute (KBSI), Daejeon 305-806, South Korea
[8]Biological Disaster Analysis Group, Korea Basic Science Institute (KBSI), Daejeon 305-806, Korea
[9]Institute of Genetics and Biophysics, Adriano Buzzati-Traverso, Via Pietro Castellino 111, 80131 Napoli, Italy
[10]IRCCS Neuromed, Pozzilli, IS 86077, Italy
[11]Institut de Biologie Valrose, University of Nice Sophia Antipolis, UMR UNS/CNRS 7277/INSERM 1091, Nice 06108, France
[12]Laboratory for Molecular and Developmental Biology, Institute for Protein Research, Osaka University, 3-2 Yamadaoka, Suita, Osaka 565-0871, Japan
[13]AMED-CREST, Japan Agency for Medical Research and Development, Tokyo 100-0004, Japan
*Correspondence: jinwookim@kaist.ac.kr
http://dx.doi.org/10.1016/j.celrep.2015.09.075

SUMMARY

***OTX2* (orthodenticle homeobox 2) haplodeficiency causes diverse defects in mammalian visual systems ranging from retinal dysfunction to anophthalmia. We find that the retinal dystrophy of *Otx2*$^{+/GFP}$ heterozygous knockin mice is mainly due to the loss of bipolar cells and consequent deficits in retinal activity. Among bipolar cell types, OFF-cone bipolar subsets, which lack autonomous *Otx2* gene expression but receive Otx2 proteins from photoreceptors, degenerate most rapidly in *Otx2*$^{+/GFP}$ mouse retinas, suggesting a neuroprotective effect of the imported Otx2 protein. In support of this hypothesis, retinal dystrophy in *Otx2*$^{+/GFP}$ mice is prevented by intraocular injection of Otx2 protein, which localizes to the mitochondria of bipolar cells and facilitates ATP synthesis as a part of mitochondrial ATP synthase complex. Taken together, our findings demonstrate a mitochondrial function for Otx2 and suggest a potential therapeutic application of OTX2 protein delivery in human retinal dystrophy.**

INTRODUCTION

OTX2 (orthodenticle homeobox 2) is a homeodomain transcription factor that supports the development of fore- and midbrain structures (Simeone et al., 2002). Homozygous loss of the *OTX2* gene yields embryos that fail to develop the head and brain in various organisms ranging from insects to humans (Acampora et al., 1995; Matsuo et al., 1995; Schröder, 2003; Wieschaus et al., 1984). Most heterozygous human *OTX2* mutations, however, do not cause apparent morphological defects in fore- or midbrain structures. Instead, they are associated with morphological defects in the eye (e.g., anophthalmia and microphthalmia) or functional impairment, such as retinal dystrophy and nyctalopia, suggesting that the development and maintenance of human visual system are *OTX2* dose and activity sensitive (Henderson et al., 2009; Ragge et al., 2005; Wyatt et al., 2008).

In the mouse eye, *Otx2* expression is observed from embryonic development to adulthood. It starts in the dorsal optic vesicle and is later restricted to the retinal pigment epithelium (RPE) and retinal neurons (Bovolenta et al., 1997; Martinez-Morales et al., 2001). In the embryonic retina, *Otx2* is expressed in post-mitotic retinal progenitor cell (RPC) daughters, where it promotes their differentiation into photoreceptors and bipolar cells by inducing key cell-fate-determining genes, such as Crx (Cone-rod homeobox containing gene) in photoreceptors and protein kinase C-α (PKC-α) in rod bipolar cells (Koike et al., 2007; Nishida et al., 2003). Therefore, photoreceptors and bipolar cells fail to develop in mice subjected to specific *Otx2* deletion in the retina (Sato et al., 2007). In addition to determining the fate of retinal neurons, Otx2 also regulates synaptogenesis through the expression of Pikachurin, an autocrine protein that binds β-dystroglycan in the presynaptic area of photoreceptors (Omori et al., 2011; Sato et al., 2008). In the adult mouse eye, *Otx2* is consistently expressed in photoreceptors, bipolar cells, and RPE. Homozygous loss of *Otx2* in adult mice results in photoreceptor degeneration, which was

proposed as a non-cell autonomous event resulting from the loss of Otx2 target gene expression in RPE (Béby et al., 2010; Housset et al., 2013).

Given the critical role of *OTX2* in human eye morphogenesis and retinal function, it is surprising that *Otx2* heterozygous mice present morphological abnormalities of the eyes only in a certain genetic background and at very low penetrance (Hide et al., 2002; Koike et al., 2007; Sugiyama et al., 2008). This suggests that *OTX2* haplodeficiency in humans and mice may affect retinal functions without modifying eye morphogenesis. Indeed, we recently found that a hypomorphic *Otx2* allele or deletions of *Otx2* resulted in retinal dystrophy in adult mice but did not affect eye morphogenesis (Bernard et al., 2014).

RESULTS

Bipolar Cells Are the Main Cell Population Affected by *Otx2* Haplodeficiency

As mammalian visual function is highly sensitive to *Otx2* gene dosage and protein activity (Bernard et al., 2014; Henderson et al., 2009; Ragge et al., 2005), it is likely that retinal dysfunction in humans and mice heterozygous for this gene reflects that the concentration of active Otx2 has decreased below a critical threshold level. Consistent with this hypothesis, we found that Otx2 mRNA and protein levels in P90 $Otx2^{+/GFP}$ heterozygous mouse retinas were less than a half of those observed in $Otx2^{+/+}$ littermate control levels (Figure S1A). The intensities of Otx2 immunostaining signals per individual outer nuclear layer (ONL) and inner nuclear layer (INL) cell of the $Otx2^{+/GFP}$ mouse retina were also decreased to 65.6% ± 5% and 54.9% ± 6% of the $Otx2^{+/+}$ values, respectively (Figures S1B [magnified images of regions indicated by dotted boxes] and S1C). Notably, the numbers of Otx2-positive cells were decreased in the INL of $Otx2^{+/GFP}$ mouse retinas, contributing additionally to the decrease in the total Otx2 level exceeding the per-cell change (Figure S1D). In contrast, the numbers of Otx2-positive cells were similar in the ONL and ganglion cell layer (GCL) (Figure S1D), which started to show degeneration after 6 months (Figure S2).

Among cells comprising the INL of P90 $Otx2^{+/GFP}$ mice, the numbers of bipolar and horizontal cells were significantly decreased, whereas the numbers of amacrine cells and Müller glial cells were not different compared with $Otx2^{+/+}$ mice (Figures S3A and S3B). To correlate the loss of the INL cells with *Otx2* expression, we compared the expression of GFP from the inactivated *Otx2* allele in the $Otx2^{+/GFP}$ mice with the expressions of various retinal markers. GFP-positive cells in the INL were mostly positive for the bipolar cell marker Vsx2 (Visual system homeobox 2), but not for the horizontal cell marker Calbindin (Figure S3A). This confirmed the previous findings that the majority of *Otx2*-expressing cells in the INL are bipolar cells (Koike et al., 2007; Nishida et al., 2003). Compared to their $Otx2^{+/+}$ littermates, $Otx2^{+/GFP}$ mice showed a 48.7% reduction in the number of Vsx2-positive bipolar cells, a decrease similar to that of Otx2-positive INL cells (Figures S1D and S3B). These results suggest that the significant deficits seen in electroretinogram (ERG) b-waves in $Otx2^{+/GFP}$ mice and a human patient with heterozygous *OTX2* mutation were caused by the loss of bipolar cells, but not Müller glial cells among which are responsible for ERG b-wave generation (Miura et al., 2009) (Figure S4).

Otx2 Haplodeficiency Exerts a Subtype-Specific Influence on Bipolar Cell Development and Degeneration

To further examine the bipolar cell loss see in $Otx2^{+/GFP}$ mice, we next investigated the distribution of bipolar subtypes in $Otx2^{+/+}$ and $Otx2^{+/GFP}$ littermate mouse retinas. Immunolabeling of all ON-type bipolar cells for G0α (G protein 0-α) revealed that P90 $Otx2^{+/GFP}$ mouse retinas contained 61.4% of such cells compared with $Otx2^{+/+}$ littermate retinas (Figures 1A [second left column] and 1B). Similarly, the percentage of PKC-α-positive rod bipolar cells, which are also an ON-type cell, was decreased to 63.5% of the $Otx2^{+/+}$ value (Figures 1A [left column] and 1B), indicating an equivalent decrease in both ON-rod and ON-cone bipolar cells in the $Otx2^{+/GFP}$ mouse retina.

A greater loss was seen among OFF-cone bipolar cells in P90 $Otx2^{+/GFP}$ mouse retinas, which harbored only 31% Vsx1-positive OFF-cone bipolar cells compared to littermate $Otx2^{+/+}$ retinas (Figures 1A [center column] and 1B). Moreover, Recoverin- and Bhlhb5 (Basic helix-loop-helix b5)-positive type II (T2) OFF-cone bipolar cells were almost absent in P90 $Otx2^{+/GFP}$ mice (Figures 1A [right two columns] and 1B). These results suggested that OFF-cone bipolar cells are more sensitive to *Otx2* haplodeficiency than ON-type bipolar cells. Consistent with these anatomical changes, the OFF responses of P90 $Otx2^{+/GFP}$ mouse retinas were remarkably decreased, and 29% of them even failed to provide OFF responses, while ON responses of the retinas were still grossly indistinguishable from those of $Otx2^{+/+}$ retinas (Figures 1C and 1D). $Otx2^{+/GFP}$ mouse retinas were also almost entirely lacking in retinal ganglion cells (RGCs) showing an ON inhibitory response, which is generated by OFF-cone bipolar cells (Figures 1E and 1F).

To investigate whether the decrease of bipolar cells in the $Otx2^{+/GFP}$ mouse retina is a developmental event as been proposed in a previous study (Koike et al., 2007), we examined the number of bipolar cells in mice at postnatal day 13 (P13), when retinal development is completed (Young, 1984, 1985). At P13, the numbers of Otx2-positive INL cells and Vsx2-positive bipolar cells in $Otx2^{+/GFP}$ mice were already reduced to 67.7% and 67.4% compared to those in $Otx2^{+/+}$ littermates (Figures 2A [top two rows] and 2B). Similar decreases were also observed in rod and ON-cone bipolar cells at P13 in $Otx2^{+/GFP}$ mice (Figures 2A [third and fourth rows] and 2B). These values were not substantially different from those at P90 (Figure 1B), indicating that rod and ON-cone bipolar cells exhibited only a mild degree of degeneration between P13 and P90. Degeneration of ON-type bipolar cells, however, progressed steadily in $Otx2^{+/GFP}$ mouse retinas, which lose ~80% of such cells by 1 year of age (Figure S5).

The number of Vsx1-positive OFF-cone bipolar cells in P13 $Otx2^{+/GFP}$ mice was about 67% of that seen in $Otx2^{+/+}$ littermate controls (Figures 2A [fifth row] and 2B), implying that about half of these cells would disappear over the following 10 weeks by P90 (Figure 1B; Figure S5). Interestingly, in P13 $Otx2^{+/GFP}$ mice, the numbers of T2 OFF-cone bipolar cells, which showed the greatest reduction at P90 (Figure 1B), were not different from those in $Otx2^{+/+}$ littermate controls (Figures 2A [bottom row] and 2B).

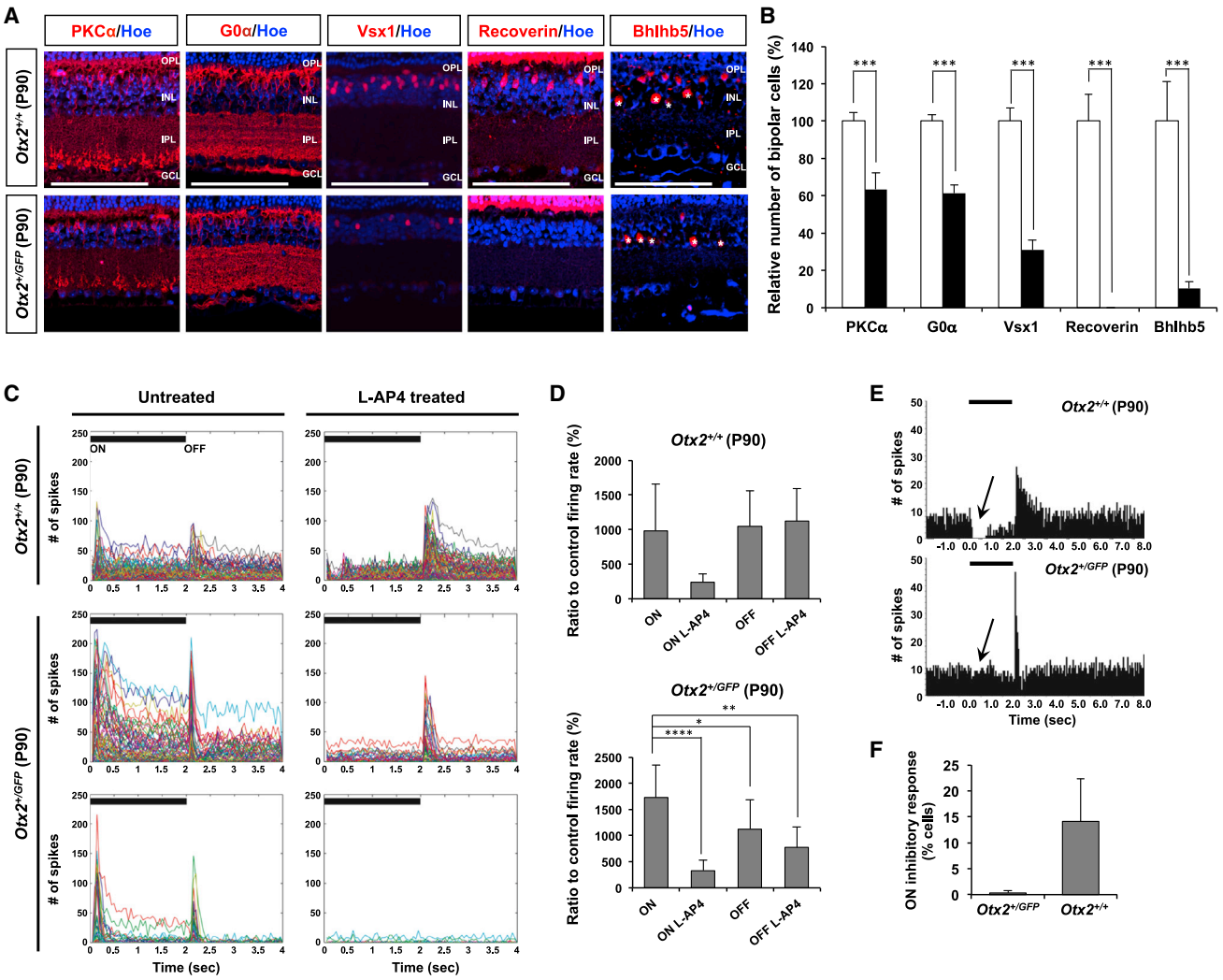

Figure 1. Subtype-Specific Degeneration Retinal Bipolar Cells upon *Otx2* Haplodeficiency

(A) Types of bipolar cells lost in P90 *Otx2*$^{+/GFP}$ mouse retinas were investigated by immunodetection of PKC-α (rod bipolar cells), G0α (ON-cone bipolar cells), Vsx1 (OFF-cone bipolar cells), Recoverin (T2 OFF-cone bipolar cells), or Bhlhb5 (OFF-cone bipolar cell subsets including T2 [Feng et al., 2006]). *Bhlhb5-positive amacrine cells.

(B) Ratios of bipolar cell subtypes in P90 *Otx2*$^{+/GFP}$ retinas (black bars) relative to those in *Otx2*$^{+/+}$ littermates (white bars) are shown graphically. Error bars are standard deviations (SD) obtained from six different samples of three independent litters. Scale bars in all images, 100 μm. All sections analyzed were obtained from samples embedded in paraffin.

(C) Light responses of P90 *Otx2*$^{+/+}$ and *Otx2*$^{+/GFP}$ mouse retina were measured by multielectrode array (MAE) in the presence or absence of mGluR antagonist L-AP4 that removes transient ON response of the retina (see Experimental Procedures for details). The graphs show peristimulus time histogram (PSTH) of RGCs in a retina. The graphs represent for *Otx2*$^{+/+}$ mouse retina (top, n = 4), *Otx2*$^{+/GFP}$ mouse retina with OFF response (middle, n = 5), and *Otx2*$^{+/GFP}$ mouse retina without OFF response (bottom, n = 2). The black bars in the graphs represent the light stimuli.

(D) Light responses of *Otx2*$^{+/+}$ and *Otx2*$^{+/GFP}$ mouse retinas were compared after normalizing the amplitudes of light response to control firing rate. Error bars denote SD; significance of difference was obtained by D'Agostino and Pearson omnibus normality test followed by one-way ANOVA + Sidak's multiple comparisons test (*95% CI of difference is between 74.07 and 1,515; **95% CI of difference is between 232.8 and 1,674; ****95% CI of difference is between 673.5 and 2,115).

(E) PSTH of single cell in the L-AP4-treated *Otx2*$^{+/+}$ (top right in C) and *Otx2*$^{+/GFP}$ (middle right in C) retina was analyzed by Spike2 software.

(F) Only 0.3% of *Otx2*$^{+/GFP}$ retinal cells show an ON inhibitory response (area indicated by arrows in E), which is detectable in 14.1% of *Otx2*$^{+/+}$ retinal cells, suggesting the loss of sustained OFF bipolar cell pathway in the *Otx2*$^{+/GFP}$ mouse retina.

These results therefore imply that the loss of OFF-cone bipolar cells, represented by T2 OFF-cone subtype, in *Otx2*$^{+/GFP}$ mice is primarily caused by degeneration, whereas the decreases in rod and ON-cone bipolar cells reflect dysgenesis and gradual degeneration during aging.

Intercellular Transfer of Otx2 from Photoreceptors to Bipolar Cells

Unexpectedly, our comparison of GFP and bipolar cell marker distributions in the INL of P13 *Otx2*$^{+/GFP}$ mouse retinas showed that the T2 OFF-cone bipolar cell marker Recoverin did not

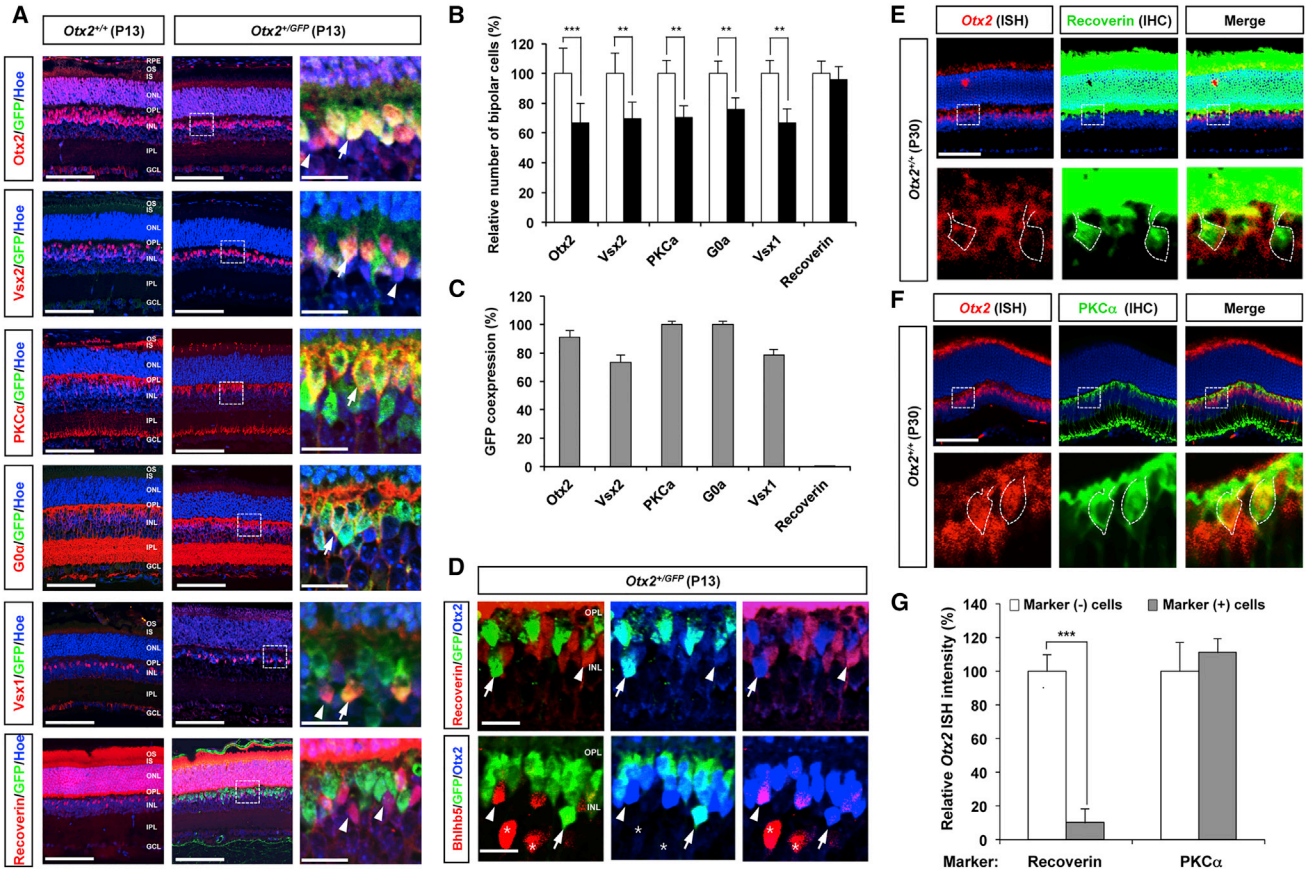

Figure 2. Presence of Exogenous Otx2 Protein in Type 2 OFF-Cone Bipolar Cells

(A) Development of bipolar cell subtypes was determined by immunostaining P13 mouse retinal sections (paraffin-embedded, 5 μm) with anti-PKC-α, anti-G0α, anti-Vsx1, or anti-Recoverin antibody, as well as by detecting Otx2-expressing cells and Vsx2-expressing pan-bipolar cells in the sections. Arrows and arrowheads indicate examples of GFP co-expressing bipolar cells and GFP-negative bipolar cells, respectively. Scale bars, 100 μm (left two columns) and 20 μm (right column).

(B) The numbers of each subset of bipolar cell in P13 *Otx2*$^{+/GFP}$ mouse retinas (black bars) were compared with those in *Otx2*$^{+/+}$ littermates (white bars), and the relative ratios were presented in a graph. Error bars, SD (**$p < 0.01$; ***$p < 0.001$).

(C) The population of bipolar cells that co-expresses GFP in each bipolar subtype is also shown graphically. Values in (B) and (C) are averages of four different retinas from three independent litters.

(D) Top, P13 *Otx2*$^{+/GFP}$ mouse retinal sections were co-stained with Alexa-647-conjugated rabbit anti-Otx2 antibody (blue), Alexa-568-conjugated rabbit anti-Recoverin antibody (red), and mouse anti-GFP antibody detected with Alexa-488-conjugated anti-mouse secondary antibody (green). Bottom, P13 *Otx2*$^{+/GFP}$ mouse retinal sections were co-stained with rabbit anti-Otx2 antibody (blue), goat anti-Bhlhb5 antibody (red), and mouse anti-GFP antibody (green) to detect Otx2 co-expressed with Bhlhb5. The arrowhead indicates a GFP-negative, Recoverin-, or Bhlhb5-positive T2 OFF-cone bipolar cell that is positive for Otx2 immunoreactivity, whereas the arrow marks a GFP-positive, Recoverin-, or Bhlhb5-negative cell that expresses Otx2. *Bhlhb5-positive amacrine cells. Scale bars, 20 μm.

(E and F) Expression of *Otx2* mRNA in P30 *Otx2*$^{+/+}$ mouse retina was examined by in situ hybridization (ISH) with digoxigenin (DIG)-labeled *Otx2* sense or *Otx2* antisense (*Otx2*) RNA probes. The RNA probes bound on the retinal sections were then visualized by HNPP fluorescence produced by alkaline phosphatase (AP)-conjugated anti-DIG antibody (Roche). HNPP fluorescence reflecting *Otx2* mRNA distribution in the retinal sections was also compared with co-immunostained T2 OFF-cone bipolar cell marker Recoverin (E) or rod bipolar cell marker PKC-α (F) by confocal microscopy.

(G) The image pixels of HNPP fluorescence in these marker-positive and -negative cells were measured by ImageJ software and shown in a graph. Values are the average obtained from 38 (Recoverin[+]), 72 (Recoverin[–]), 50 (PKC-α[+]), and 53 (PKC-α [–]) cells in three sections from two independent eyes. Error bars, SD; ***$p < 0.001$. Scale bars, 100 μm.

overlap with the GFP signal, whereas rod and ON-cone bipolar cells co-expressed GFP and their specific markers, PKC-α and G0α, respectively (Figures 2A [right column] and 2C). More strikingly, GFP-negative T2 OFF-cone bipolar cells, which were positive for Recoverin and Bhlhb5, contained Otx2 (arrowheads in Figure 2D). The transcription-independent expression of Otx2 in T2 OFF-cone bipolar cells was further proved by the lack of *Otx2* mRNA in these cells (Figures 2E and 2F). Our results therefore suggest that Otx2 was transferred into T2 OFF-cone bipolar cells from an external source, perhaps similar to the intercellular transfer of Otx2 from the choroid plexus to cortical parvalbumin (PV) neurons (Spatazza et al., 2013; Sugiyama et al., 2008).

In the mouse retina, photoreceptors and bipolar cells express *Otx2* (Koike et al., 2007; Nishida et al., 2003). Thus, these cells

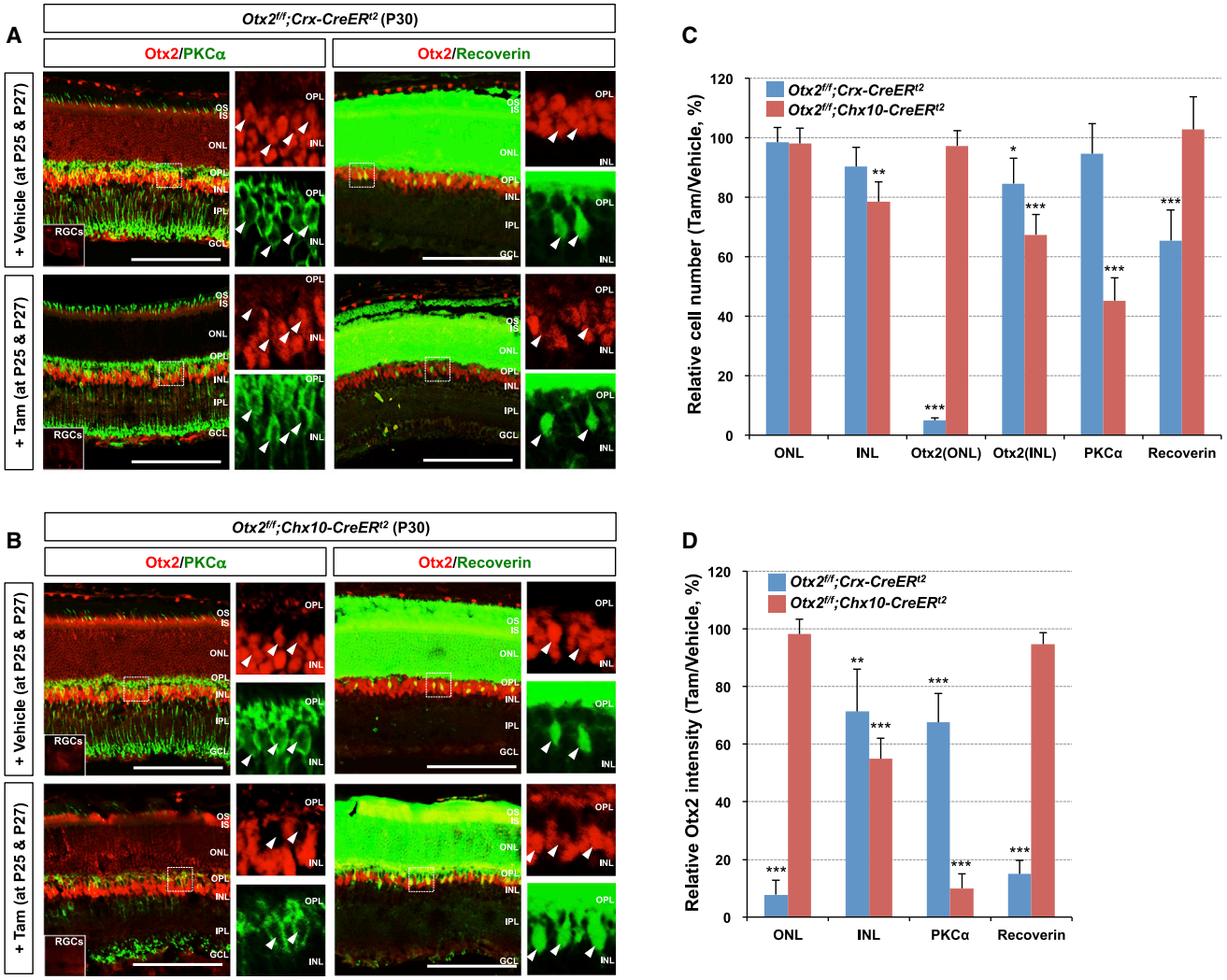

Figure 3. Intercellular Transfer of Otx2 from Photoreceptor to Bipolar Cells

(A and B) Exon 2 of *Otx2* gene flanked by two loxP sites was deleted specifically in photoreceptors (*Otx2*$^{f/f}$*;Crx-CreER*^{t2}, A) or bipolar cells (*Otx2*$^{f/f}$*;Chx10-CreER*^{t2}, B) by Cre-ER^{t2} recombinases, which were activated by two repeated injections of tamoxifen at P25 and P27. Then, distribution of Otx2 in the retinal neurons of P30 mice was examined by co-immunostaining of Otx2 and corresponding bipolar cell markers. Scale bars, 100 μm.

(C) Relative numbers of total ONL cells, total INL cells; Otx2-positive cells in ONL and INL; PKC-α-positive rod bipolar cells; and Recoverin-positive T2 OFF-cone bipolar cells in the retinas were counted and shown in a graph.

(D) Intensity of Otx2 immunostaining signal in corresponding cells in the mouse retinas were measured by ImageJ software and presented mean values in a graph. The scores in (C) and (D) are average values of five retinas from two independent litters. *p < 0.05; **p < 0.01; ***p < 0.001.

could be the potential sources for exogenous Otx2 observed in T2 OFF-cone bipolar cells. To test this possibility, we generated *Otx2*$^{f/f}$*;Crx-CreER*^{t2} and *Otx2*$^{f/f}$*;Chx10-CreER*^{t2} mice, in which *Otx2* was specifically eliminated in adult photoreceptors and bipolar cells, respectively. In these mice, CreER^{t2} recombinases became active to delete exon 2 of *Otx2* in photoreceptors and bipolar cells upon binding with the estrogen analog tamoxifen (Fossat et al., 2006). In P30 *Otx2*$^{f/f}$*;Crx-CreER*^{t2} mice, which were exposed to tamoxifen by two repeated intraperitoneal injections at P25 and P27, Otx2 immunostaining signals were disappeared specifically from photoreceptors (Figure 3A, left column). The number of ONL cells was not greatly different between tamoxifen-injected and vehicle-injected *Otx2*$^{f/f}$*;Crx-CreER*^{t2} mouse retinas at day 5 post-injection (Figure 3C), suggesting that photoreceptors did not degenerate upon the loss of *Otx2* at this point. In contrast, the number of T2 OFF-cone bipolar cells was decreased by 65.5% in the tamoxifen-injected *Otx2*$^{f/f}$*;Crx-CreER*^{t2} mice, whereas the numbers of rod bipolar cells was not altered significantly (Figures 3A and 3C). Moreover, the average Otx2 intensity in Recoverin-positive T2 OFF-cone bipolar cells in the tamoxifen-injected *Otx2*$^{f/f}$*;Crx-CreER*^{t2} mouse retinas was also decreased to 15% of that seen in the vehicle-treated group (Figures 3A and 3D). PKC-α-positive rod bipolar cells in the tamoxifen-injected *Otx2*$^{f/f}$*;Crx-CreER*^{t2} mouse retinas

retained Otx2 proteins at 67.6% of the level observed in vehicle-injected *Otx2$^{f/f}$;Crx-CreER^{t2}* mouse retinas (Figures 3A and 3D), suggesting that both T2 OFF-cone bipolar cells and rod bipolar cells possess Otx2 derived from photoreceptors.

In tamoxifen-injected P30 *Otx2$^{f/f}$;Chx10-CreER^{t2}* mouse retinas, Otx2 was significantly lost from rod bipolar cells, which were decreased by half compared to the number seen in the vehicle-treated group (Figures 3B–3D). However, the number of T2 OFF-cone bipolar cells and the signal intensity of Otx2 in the cells did not differ greatly between tamoxifen- and vehicle-treated P30 *Otx2$^{f/f}$;Chx10-CreER^{t2}* mouse retinas (Figures 3B–3D). The level of Otx2 in RGCs was decreased significantly in the *Otx2$^{f/f}$;Chx10-CreER^{t2}* mouse retina, however, reaffirming that the bipolar cells are the source of the Otx2 detected in RGCs (Sugiyama et al., 2008) (Figures 3A and 3C, insets in left column). Together, these results suggested that the exogenous Otx2 in T2 OFF-cone bipolar cells is mainly derived from photoreceptors. The results also indicate that the photoreceptor-derived Otx2 is more critical for the survival of T2 OFF-cone bipolar cells, which are absence of endogenous Otx2 expression, than that of rod bipolar cells, which can express Otx2 endogenously (Figure 2F).

Intraocular Otx2 Injection Restores Bipolar Cells and Retinal Activity in *Otx2$^{+/GFP}$* Mice

The intriguing presence of exogenous Otx2 in bipolar cells and the reduced amount of exogenous Otx2 in rapidly degenerating T2 OFF-cone bipolar cells in *Otx2$^{+/GFP}$* mice prompted us to hypothesize that the imported Otx2 exerts a protective effect in the bipolar cells. To test this possibility, we augmented extracellular Otx2 levels by injecting recombinant Otx2-myc protein intravitreally into the right eyes of *Otx2$^{+/GFP}$* mice at P13 (the Müller glial end-feet barrier is not completely formed at this point, giving the protein access to the retinal neurons [Figure S6A]). To investigate the effects of Otx2 injection on the retinal dystrophy induced by *Otx2* haplodeficiency, we first compared the ERG responses of *Otx2$^{+/GFP}$* mice between Otx2-injected right eyes and left eyes injected with PBS or cell-penetration-defective Otx2^{YL}-myc protein (Sugiyama et al., 2008). We found that injection of Otx2-myc, but not PBS or Otx2^{YL}-myc, restored ERG responses in the eyes of P30 *Otx2$^{+/GFP}$* mice to nearly *Otx2$^{+/+}$* levels, even though the protein stayed in the retinal neurons for less than a week (Figure 4A–4C; Figure S6B). We also examined the numbers of bipolar cells in Otx2-injected right eyes compared with control PBS- or Otx2^{YL}-injected left eyes of the same animals. Our results revealed that numbers of T2 OFF-cone bipolar cells and rod bipolar cells in the Otx2-injected right eyes of *Otx2$^{+/GFP}$* mice were increased to levels similar to those observed in P13 *Otx2$^{+/GFP}$* mice (Figure 4D). Thus, the survival of bipolar cells appears to require the presence of a critical amount of exogenously derived Otx2 protein. This is especially true for T2 OFF-cone bipolar cells, which do not express *Otx2* and depend on imported Otx2 for their survival.

Mitochondrial Localization of Exogenous Otx2 in Retinal Neurons

Although a previous report showed that exogenous Otx2 has a protective activity in RGCs (Torero Ibad et al., 2011), the underlying mechanism remained unknown. Interestingly, a significant portion of the exogenously derived Otx2 in bipolar cells and RGCs was distributed in the cytoplasm (Figures S1B and S6), suggesting that exogenously derived Otx2 may function in this compartment. Furthermore, externally provided Otx2-myc protein was not evenly diffused in cultured retinal RGC5 cells (Nieto et al., 2011), but rather formed puncta in the cytoplasm (Figure 5A). Comparison of exogenous Otx2-myc with the distribution of markers for various cellular organelles revealed that the cytoplasmic Otx2-myc signal substantially overlapped with that of the mitochondrial marker, Tom20 (Translocase of outer mitochondrial membrane 20), but not with the Golgi marker, GM130, or the lysosomal protein, Lamp2a (Lysosomal-associated membrane protein 2a) (Figure 5A).

Exogenous Otx2 was also found to be localized to mitochondria in mouse retina. Infused Otx2-myc co-localized with Tom20 at the OPL post-synaptic area, which primarily consists of bipolar cells (Figure 5B). Electron microscopic analyses of myc-immunostained retinal sections further revealed that injected Otx2-myc was preferentially located in mitochondria at the OPL post-synaptic area (Figures 5C and 5D). Endogenously expressed Otx2 also co-localized with Tom20 in P14 mouse retinal RGCs and bipolar cells (Figure 5E). We also detected Otx2 in mitochondria isolated from P14 mouse retinas (Figure 5F). The amount of Otx2 in the mitochondrial fraction was markedly decreased after disrupting hydrophilic interactions using a high-salt buffer or by degrading proteins located on the mitochondrial outer membrane with proteinase K (Figure 5F, right two lanes). These results suggest that most mitochondrial Otx2 binds to polar residues of lipids or proteins in the mitochondrial outer membrane and slowly moves inside mitochondria, via a process similar to that involved in cell penetration of Otx2 (Beurdeley et al., 2012). Recombinant Otx2-myc was also detectable in mitochondria in a cell-free system, suggesting that mitochondrial translocation is an intrinsic property of Otx2, independent of guiding factors in the cytoplasm or plasma membrane (Figure 5G).

Exogenous Otx2 Facilitates Mitochondrial ATP Synthesis

To gain new insights into the roles of mitochondrial Otx2, we set out to identify its interacting proteins in P14 retinal neurons (see details in Supplemental Experimental Procedures). We identified mitochondrial ATP synthase subunit α (Atp5a1), a F1 catalytic core component of ATP synthase comprising the mitochondrial oxidative phosphorylation (OXPHOS) complex V (Chaban et al., 2014), and solute carrier 25a31 (Slc25a31), a mitochondrial ADP/ATP translocator (Kim et al., 2007), suggesting that Otx2 may play a role in mitochondrial ATP synthesis (Table S1). We also recovered mitochondrial ATP synthase subunit-a (Mtatp6), a linker subunit of the mitochondrial ATP synthase complex, as an Otx2-binding protein, but failed to recover any other OXPHOS complex component (Figure 6A), implicating that Otx2 interacts with Atp5a1 in the ATP synthase complex. Furthermore, Otx2 was detected in a mitochondrial protein complex with a molecular weight (MW) of ~700 kDa, which is the expected MW of the OXPHOS complex V (C-V), in native

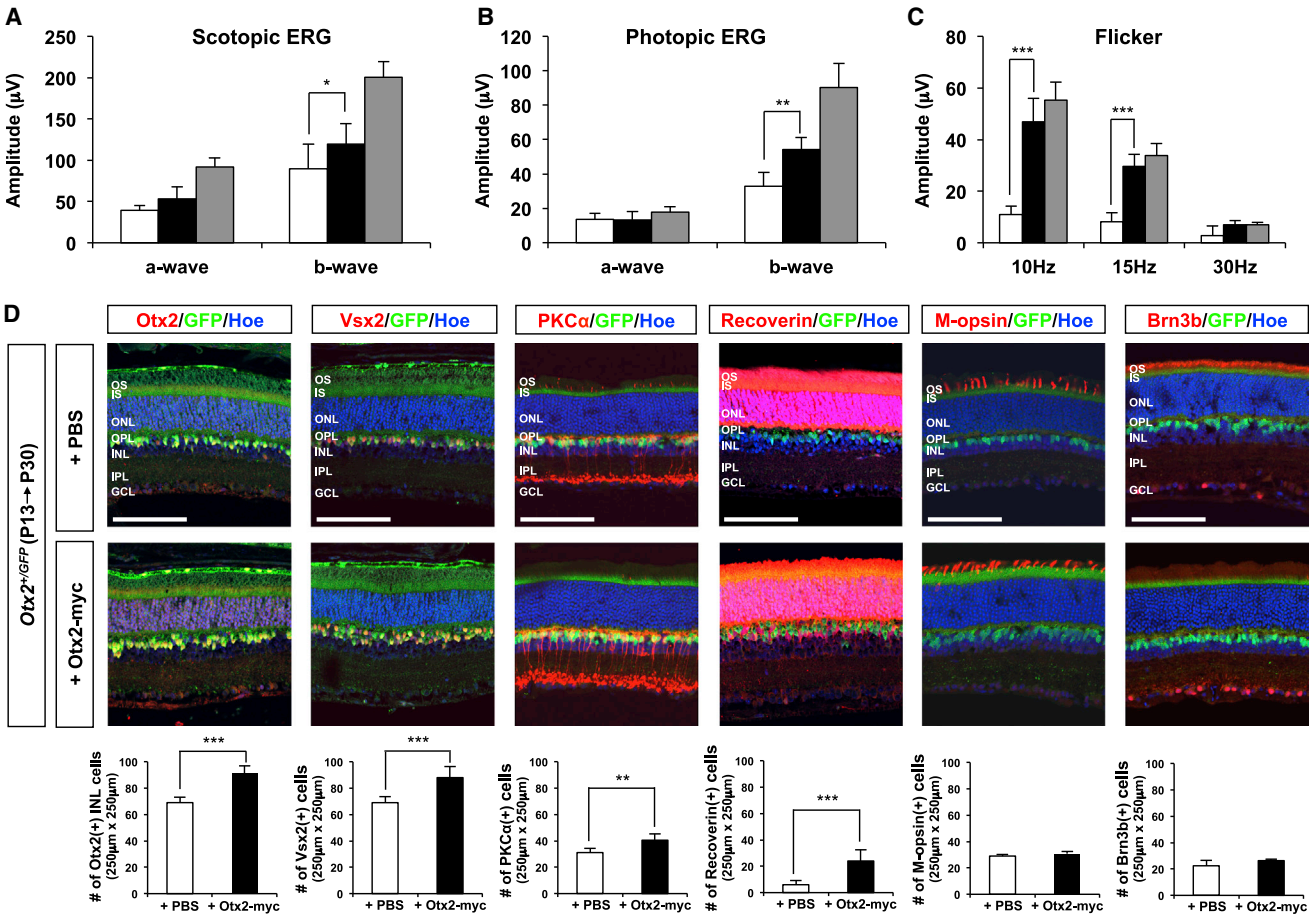

Figure 4. Intraocular Injection of Otx2 Protein Restores Retinal Activity in *Otx2*$^{+/GFP}$ Mice

(A) P13 *Otx2*$^{+/GFP}$ mice were injected with 200 ng of recombinant Otx2-myc protein (n = 6) and PBS (n = 3) or cell penetration-defective Otx2^{YL}-myc protein (200 ng; n = 3) into the intravitreal space of right and left eye, respectively. After the injection, the mice were returned to normal habitats until P29. The mice were then dark-adapted for 16 hr, and scotopic ERG responses of both eyes were assessed simultaneously at a light intensity of 2.5 cds. Average amplitudes of scotopic ERG a-waves and b-waves measured from PBS-injected left eyes (white bars) and Otx2-injected right eyes (black bars) were compared with those from uninjected *Otx2*$^{+/+}$ littermates (gray bars, n = 3).

(B and C) Photopic (B) and flicker (C) ERG responses of the mice were also measured after adapted under room light (30 cd/m^2). Error bars in (A)–(C), SD; p values obtained by ANOVA test are *p < 0.05; **p < 0.01; ***p < 0.001.

(D) Retinal sections were obtained from ERG-measured *Otx2*$^{+/GFP}$ mice for a comparison of retinal cell composition between cells PBS-injected left eyes or Otx2-injected right eyes. Cells were then evaluated for expressions of Otx2, Vsx2, PKC-α, Recoverin, M-opsin, and Brn3b by immunostaining with the corresponding antibodies. Scale bars, 100 μm. The numbers of cells expressing each marker are shown graphically (white bar, *Otx2*$^{+/+}$; black bar, *Otx2*$^{+/GFP}$). Values are averages of four different retinas from three independent experiments; error bars, SD (**p < 0.01, ***p < 0.001).

polyacrylamide gels (Figure 6B). These results suggest exogenous Otx2 may function as a member of mitochondrial OXPHOS C-V. Consistent with this notion, ATP synthesis rate of mitochondria isolated from mouse retinas showed significant elevation in the presence of Otx2-myc (Figure 6C). Taken together, these results suggest that Otx2 is a component of mitochondrial OXPHOS C-V in the mouse retina.

Despite the significant increase of mitochondrial ATP synthase activity after exogenous Otx2 addition, the distribution and number of mitochondria in the Otx2-myc-injected P15 *Otx2*$^{+/GFP}$ mouse retinas did not differ greatly from those in *Otx2*$^{+/+}$ and *Otx2*$^{+/GFP}$ littermate retinas (Figure 6D). The levels of OXPHOS complex components also did not substantially differ among those mouse retinas (Figure 6B [OXPHOS WB at right]; Figure S7). It indicates that imported Otx2 facilitates mitochondrial ATP synthesis by promoting OXPHOS C-V activity without affecting the expression of OXPHOS components. In contrast, morphologies of mitochondria in the post-synaptic area of *Otx2*$^{+/GFP}$ mouse retinal OPL neurons, which are predicted to be bipolar cells, differed from that of *Otx2*$^{+/+}$ neurons. In particular, cristae of the inner mitochondrial membrane were unfolded and disrupted in *Otx2*$^{+/GFP}$ mouse OPL post-synaptic areas (Figures 6E [middle panel] and 6F). The numbers of mitochondria with normal morphologies were increased in the post-synaptic OPL neurons of Otx2-injected *Otx2*$^{+/GFP}$ mouse eyes (Figures 6E [right panel] and 6F), suggesting that the imported Otx2 might

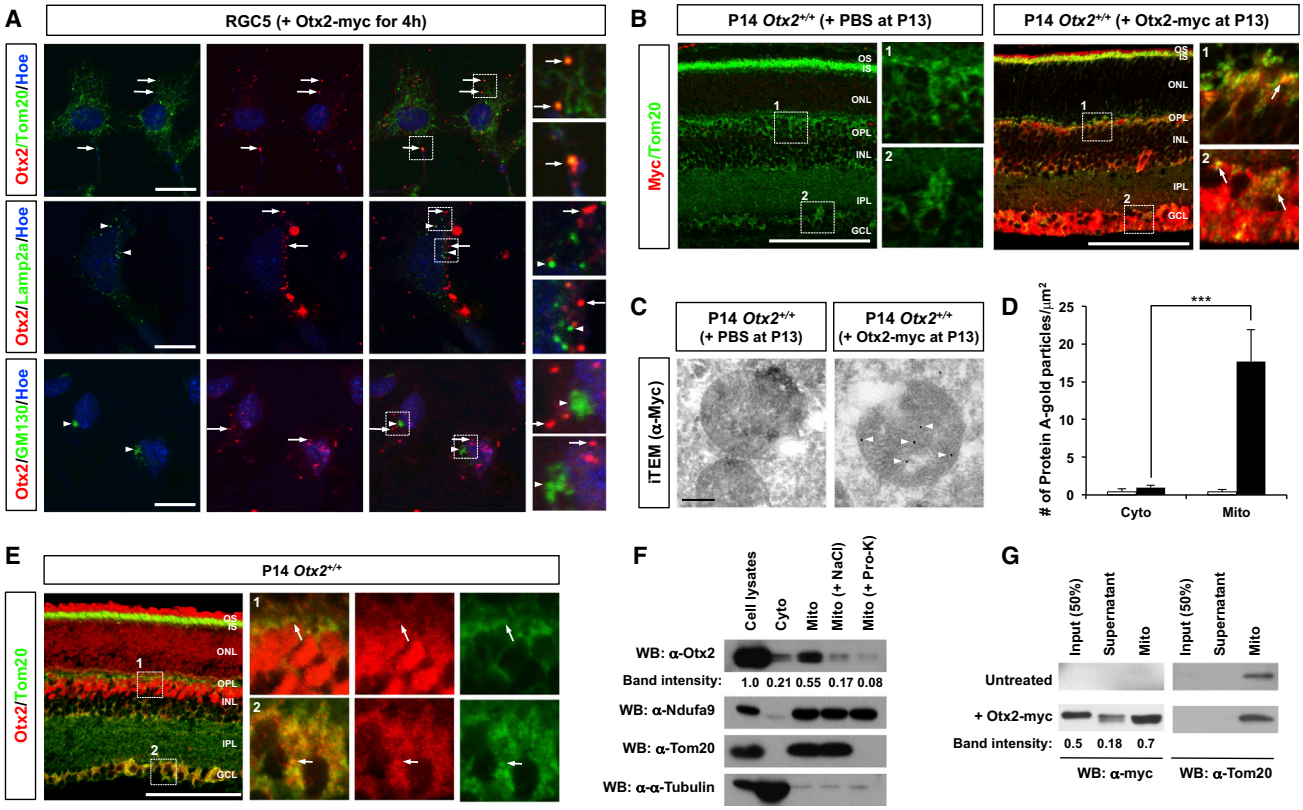

Figure 5. Mitochondrial Localization of Imported Otx2

(A) RGC5 mouse retinal cells were treated with recombinant Otx2-myc protein (10 ng/ml) for 4 hr, and intracellular locations of the Otx2-myc protein were detected by co-immunostaining with anti-Otx2 antibody and subcellular organelle markers, such as Tom20 (mitochondria), Lamp2a (lysosome), and GM130 (Golgi apparatus). Images in the right column are areas of dotted-boxes in the merged images. Scale bars, 25 μm.

(B) Mitochondrial localizations of exogenous Otx2-myc (200 ng), which was injected into intravitreal space at P13, in bipolar cells and RGCs of P15 *Otx2*$^{+/+}$ mouse retina were investigated by co-staining Otx2 (red) and Tom20 (green). Arrows indicate Otx2 co-localizing with Tom20. Scale bar, 100 μm.

(C) Otx2-myc protein (200 ng) was injected into the right eyes of P13 *Otx2*$^{+/+}$ mice, while PBS was injected into the left eyes of same mice. The eyes were enucleated and then processed as described in Experimental Procedures. The presence of the injected Otx2-myc protein in the retinal sections (70 nm) was visualized by transmission electron microscopy after immunostaining (iTEM) with rabbit anti-myc antibody and subsequent 10 nm gold-labeled protein A. White arrowheads indicate Otx2-myc proteins detected by the staining. Scale bar, 0.2 μm.

(D) Relative amounts of external Otx2-myc in mitochondria (Mito) and cytoplasm (Cyto) of PBS- or Otx2-myc-injected mouse retinal sections were indirectly measured by counting protein A-gold particles that bound to anti-myc rabbit immunoglobulin G (IgG). Nine (+PBS; white bars) and sixteen (+Otx2-myc; black bars) iTEM images taken of three retinal samples from two independent experiments were used for the counting. ***$p < 0.001$.

(E) Mitochondrial localization of endogenous Otx2 was also investigated by immunodetection of Otx2 co-localizes with Tom20 in P14 mouse retina. Image at left is a deconvoluted version of 12 different focal images, while magnified versions are those of a single focal plane.

(F) Presence of Otx2 at mitochondria was examined by centrifugal fractionation and subsequent western blotting (see details in Experimental Procedures). In a buffer with 0.5 M NaCl, the majority of hydrophilic interactions were disrupted. By treating with proteinase-K, proteins locating at mitochondrial outer membrane were degraded, while internal mitochondrial proteins remain intact. Total, total cell lysates; Cyto, cytosolic fraction; Mito, mitochondrial fraction. Ndufa9 is a marker for internal mitochondrial proteins; Tom20 is a marker for the mitochondrial outer membrane protein, and α-tubulin is a loading control. Relative intensities of Otx2 bands were measured by ImageJ software.

(G) Mitochondrial localization of Otx2-myc was investigated by incubating the protein (Input, 200 ng) with purified mitochondria (100 μg) from P14 mouse retina in PBS at 30°C for 60 min. Supernatants and mitochondrial pellets (Mito), which were washed twice with PBS, were obtained by centrifugation and analyzed by Western blot with anti-Otx2 and anti-Tom20 antibodies. Relative intensities of Otx2 bands were measured by ImageJ software.

support the mitochondrial inner membrane structure by modulating OXPHOS C-V, which has been shown to promote folding of the mitochondrial inner membrane into cristae stacks (Schultz and Chan, 2001). Due to this decrease in the structural integrity of the mitochondria, the mitochondrial transmembrane potential ($\Delta\Psi_m$) of *Otx2*$^{+/GFP}$ mouse retinal OPL was lower than those of littermate *Otx2*$^{+/+}$ and Otx2-injected *Otx2*$^{+/GFP}$ mouse retinas (Figures 6G and 6H).

Exogenous Otx2 Protects OFF-Cone Bipolar Cells from Glutamate Excitotoxicity

Mitochondria are highly concentrated in retinal synaptic areas, which are enriched for ATP-demanding molecules, including ion channels, transporters, and translational machineries (Mattson et al., 2008; Vos et al., 2010). ATP synthesized by Otx2-containing OPL post-synaptic mitochondria might not only act autonomously in bipolar cells, it could also be secreted into the

extracellular space and utilized by neighboring cells, including Müller glia that can uptake synaptic glutamate through Glast (Glutamate aspartate transporter) and convert it to glutamine using glutamine synthetase in an ATP-dependent manner (Derouiche and Rauen, 1995). In addition to impairing the ATP-dependent events in $Otx2^{+/GFP}$ mouse bipolar cells, therefore, the reduced ATP synthesis in these cells might also result in the accumulation of synaptic glutamate, which is released from photoreceptors in the dark to depolarize OFF-type bipolar cells but hyperpolarize ON-type bipolar cells (DeVries and Schwartz, 1999; Shiells et al., 1981). This could further sensitize OFF-cone bipolar cells to glutamate excitotoxicity.

To test this hypothesis, we maintained newborn $Otx2^{+/+}$ and $Otx2^{+/GFP}$ mice in the dark to induce a sustained release of glutamate from photoreceptors and excitation of post-synaptic OFF-cone bipolar cells. In these dark-reared P30 $Otx2^{+/GFP}$ mice, degeneration of T2 OFF-cone bipolar cells was accelerated compared to littermate $Otx2^{+/GFP}$ mice kept under a daily light/dark cycle (Figures 7A [the two center images] and 7B). The numbers of T2 OFF-cone bipolar cells in $Otx2^{+/+}$ mouse retinas were also reduced significantly in the dark condition (Figures 7A [two leftmost images] and 7B), whereas the numbers of rod bipolar cells in $Otx2^{+/+}$ and $Otx2^{+/GFP}$ mice did not significantly differ in dark- versus light/dark-reared mice (Figures 7C and 7D). The degeneration of T2 OFF-cone bipolar cells in the dark-reared P30 $Otx2^{+/+}$ and $Otx2^{+/GFP}$ mice was attenuated by intraocular Otx2-myc injection at P13 (Figures 7A [two right images] and 7B), suggesting that exogenous Otx2 protected the bipolar cells against dark-induced glutamate excitotoxicity.

DISCUSSION

Early onset retinal dystrophy in human and mice carry heterozygous mutations of *OTX2* is mainly related to the reduced numbers of bipolar cells (Bernard et al., 2014; Henderson et al., 2009) (Figures 1 and S3). The implication of these findings is that the effects of OTX2 are dose sensitive, with the level of OTX2 in the mutant retina failing to exceed the threshold necessary for the development and maintenance of these cells. A reduction of these cells in the human and mouse retina could arise through three possible mechanisms, which are not mutually exclusive. First, *OTX2* haplodeficiency may reduce the number of bipolar cells generated. Second, OTX2 may exert specific anti-apoptotic activity during a critical postnatal maturation period. Third, mature bipolar cells may fail to thrive in *OTX2* mutant human and mouse retinas (i.e., OTX2 may promote the survival of these cells in the adult retina). These possibilities could be tested in $Otx2^{+/GFP}$ mice.

The birth of bipolar cells in mice peaks at P3, continues at P7, and is completed by P11 (Young, 1984, 1985). The number of bipolar cells has already decreased by P13 in $Otx2^{+/GFP}$ mouse retinas (Figures 2A and 2B; Figure S5). This decrease could reflect dysgenesis, as proposed in the first possible mechanism, or by elevated apoptotic elimination, as proposed in the second. The number of Vsx2-positive bipolar cells in the INL of $Otx2^{+/GFP}$ mouse retinas was already approximately 30% less than that in $Otx2^{+/+}$ littermates at P7 (data not shown), suggesting that Otx2 supports bipolar cell development. The number of bipolar cells in $Otx2^{+/GFP}$ mice did not decrease significantly compared with $Otx2^{+/+}$ littermates during the second postnatal week (P7–P13), suggesting that apoptotic elimination did not differ between $Otx2^{+/+}$ and $Otx2^{+/GFP}$ mouse retinas during this period. Bipolar cells degenerated progressively during later stages, in a subtype-specific manner (Figure S5). Taken together, these results suggest that a full dose of *Otx2* is critical for the development (hypothesis one) and maintenance (hypothesis three) of bipolar cells, but not for post-natal elimination (hypothesis two).

However, the first hypothesis was not applicable to T2 OFF-cone bipolar cells, which did not differ in P13 $Otx2^{+/+}$ and $Otx2^{+/GFP}$ mouse retinas but later degenerated more rapidly than the other bipolar subtypes. Therefore, in contrast to ON-type bipolar cells, the maintenance (hypothesis three) but not the development (hypothesis one) of T2 OFF-cone bipolar cells is sensitive to *Otx2* haplodeficiency. More surprisingly, Otx2 was detected in T2 OFF-cone bipolar cells in the absence of endogenous *Otx2* mRNA expression, as also evidenced by the lack of GFP co-expression from the deleted *Otx2* allele (Figure 2). The levels of Otx2 in T2 OFF-cone bipolar cells were decreased in $Otx2^{f/f};CrxCreER^{t2}$ mouse retina, which lost *Otx2* in their photoreceptors for up to 5 days (Figure 3), suggesting that the Otx2 in T2 OFF-cone bipolar cells was obtained from the photoreceptors through intercellular transfer, as has been shown for cortical PV neurons that obtain Otx2 produced from the choroid plexus (Spatazza et al., 2013). In support of the cell-protective roles of exogenous Otx2, the T2 OFF-cone bipolar cells degenerated under conditions of reduced Otx2 transfer but thrived following the intraocular supplementation of exogenous Otx2 (Figures 4 and 7).

Otx2 haplodeficiency had the greatest influenced on T2 OFF-cone bipolar cells, even though exogenous Otx2 could be internalize by other types of bipolar cells (Figures 3, 5 and S6). The hypersensitivity of T2 OFF-cone bipolar cells to *Otx2* haplodeficiency might reflect relative levels of external Otx2 to total cellular Otx2. Because the Otx2 supply depends on photoreceptors, haplodeficient *Otx2* expression in the photoreceptors correspondingly resulted in the decrease of imported Otx2 in T2 OFF-cone bipolar cells to sub-threshold level. In contrast, ON-type bipolar cells contain both endogenous and exogenous Otx2 (Figure 2), suggesting that endogenous Otx2 might support the survival of ON-type bipolar cells upon decrease of Otx2 import. Future studies are warranted to investigate the potential mechanisms through which endogenous Otx2 might support the survival of ON-type bipolar cells.

The regulation of mitochondrial activity by a homeodomain protein was previously shown for En2, which protects dopaminergic neurons in a mouse model of Parkinson's disease by enhancing the translation of mRNA for the mitochondrial OXPHOS C-I component Ndufs (NADH dehydrogenase [ubiquinone] iron-sulfur proteins) (Alvarez-Fischer et al., 2011). En2 also stimulates RGC axon growth by increasing the local synthesis of Lamin B2, which associates with mitochondria (Yoon et al., 2012). The levels of Ndufs1 (but not Ndufs3 or Ndufa1) and Lamin B2 in $Otx2^{+/GFP}$ mouse retinas were reduced in comparison to those in $Otx2^{+/+}$ littermate retinas (Figure 7; Lamin B2 data not shown), suggesting that Otx2 regulates mitochondrial activity

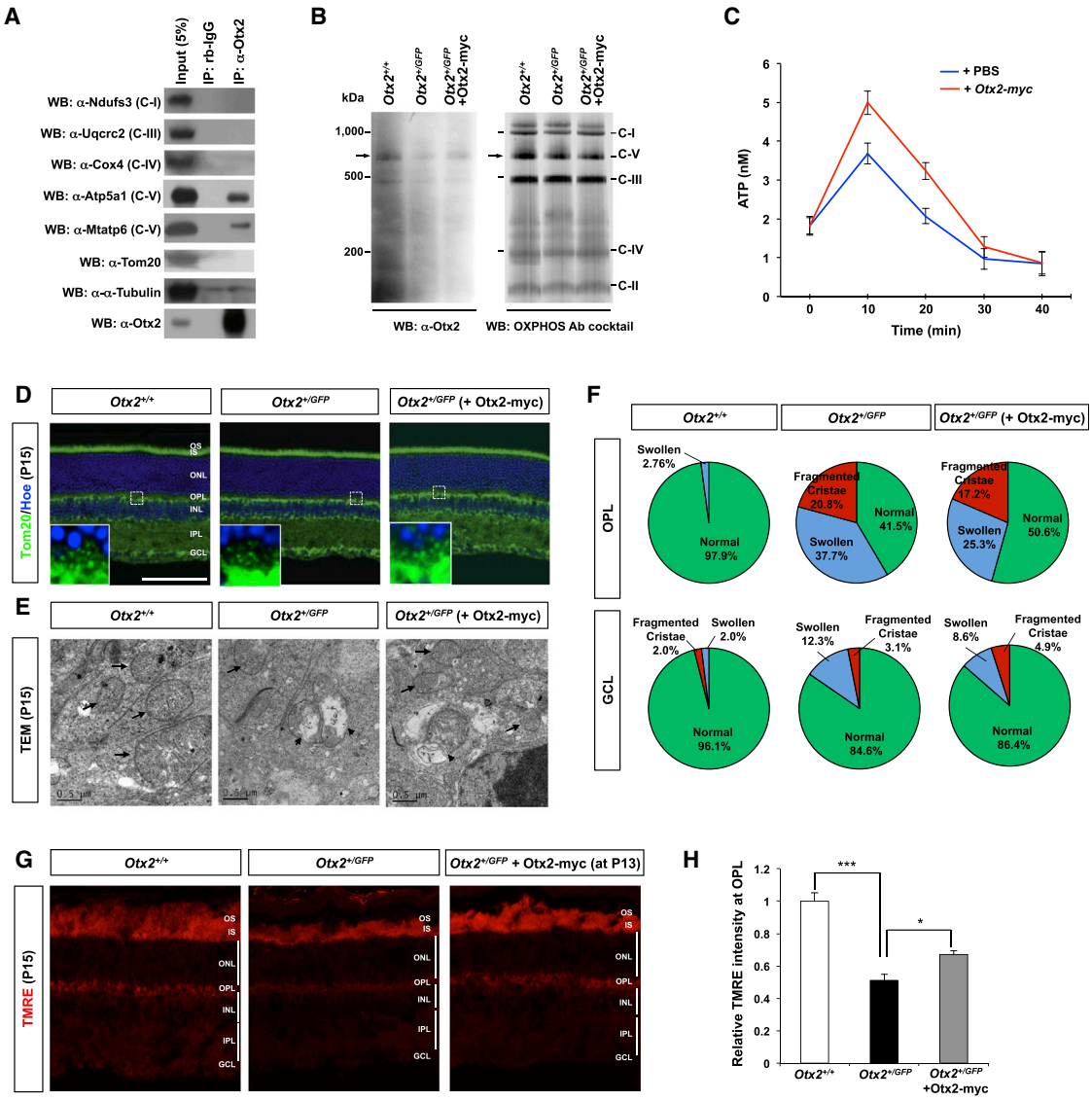

Figure 6. Exogenous Otx2 Protein Is a Component of Mitochondrial ATP Synthase

(A) Interaction between Otx2 and Atp5a1 in mitochondrial fraction of P14 mouse retinal cells was proven by immunoprecipitation with rabbit anti-Otx2 antibody. Co-purification of other mitochondrial OXPHOS complex components, a mitochondrial outer membrane protein Tom20, and a cytoplasmic protein α-tubulin was also evaluated by western blotting with corresponding antibodies. Non-specific pull-downs of the proteins were also checked by immunoprecipitation with preimmune rabbit IgG (rb-IgG).

(B) Presence of Otx2 in native mitochondrial protein complexes in P15 $Otx2^{+/+}$, $Otx2^{+/GFP}$, or Otx2-injected $Otx2^{+/GFP}$ mouse retinas was examined by duplicated BN-PAGE gels, one of which was analyzed by western blotting with anti-Otx2 antibody (left), while the other was detected by Anti-OxPhos Complex Kit (Invitrogen, right). Size of mitochondrial Otx2 protein complex was then compared with those of OXPHOS complexes. Relative intensities of Otx2 and OXPHOS complex V (C-V; detected by anti-Atp5a1 antibody) bands were measured by ImageJ software (n = 3 for Otx2; n = 4 for OXPHOS complexes). The values are average obtained from three independent experiments. The values following to ± are SD. *p* values of Otx2 band intensities are <0.01 ($Otx2^{+/+}$ versus $Otx2^{+/GFP}$) and <0.05 ($Otx2^{+/+}$ versus $Otx2^{+/GFP}$+Otx2-myc).

(C) The effects of Otx2 on mitochondrial ATP synthesis were accessed by incubating mitochondria, which were purified from P14 $Otx2^{+/+}$ mouse retinas, in the presence or absence of Otx2-myc/His (0.5 μg/ml) for indicated time periods (see details in Experimental Procedures). The values are the average obtained from four independent measurements. Error bars, SD.

(D) Distribution of mitochondria in P15 retinas of $Otx2^{+/+}$ mice, $Otx2^{+/GFP}$ mice, and $Otx2^{+/GFP}$ mice injected with Otx2 (200 ng/eye) at P13 were visualized by immunostaining detecting mitochondrial protein Tom20. Scale bars, 100 μm.

(E) Ultrastructures of mitochondria at post-synaptic areas of OPL of these mouse retinas were monitored by transmission electron microscopy (TEM).

(F) Numbers of mitochondria classified by morphological characteristics are shown. Mitochondria counted in OPL are $Otx2^{+/+}$ = 47, $Otx2^{+/GFP}$ = 83, and $Otx2^{+/GFP}$ + Otx2-myc = 87, while those in GCL are $Otx2^{+/+}$ = 51, $Otx2^{+/GFP}$ = 65, and $Otx2^{+/GFP}$ + Otx2-myc = 81. Numbers of retinas used for counting were three, which are analyzed in two independent experiments, for each group. Values in the graphs are averages.

(legend continued on next page)

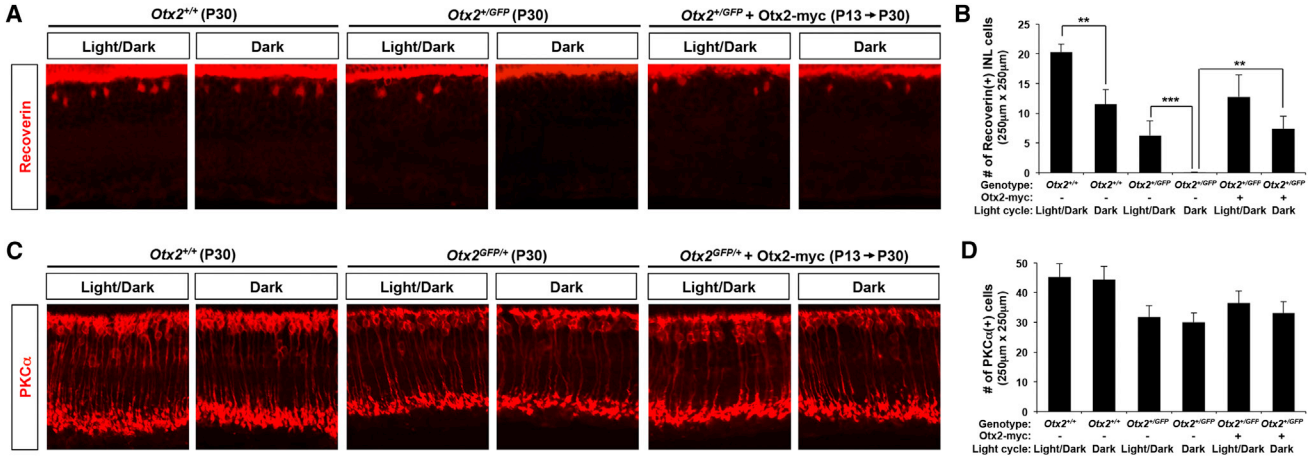

Figure 7. Otx2 Transfer to Bipolar Cell Is Protective against Glutamate Excitotoxicity

Newborn littermate *Otx2*$^{+/+}$ and *Otx2*$^{+/GFP}$ mice were maintained in dark or 12-hr-light/12-hr-dark cycle for 30 days (P30) with a brief interruption at P13 for the injection of Otx2-myc (200 ng) into the vitreal space of the mouse eyes.

(A and C) The distribution of Recoverin-positive T2 OFF-cone bipolar cells (A) and PKC-α-positive rod bipolar cells (C) in these mouse retinas was investigated by immunostaining.

(B) and (D) Values in the graphs are average numbers of detected cells in confocal images (250 × 250 μm) analyzed five retinas in two independent experiments. Scale bars, 100 μm. Error bars, SD (**p < 0.01; ***p < 0.001).

in multiple ways, including the modulation of mitochondrial protein synthesis and activation of OXPHOS C-V.

Our study shows that mice with an *Otx2* haplodeficiency have diminished visual performance and retinal dysfunction. A human patient carrying a heterozygous *OTX2* nonsense mutation was reported to have a similar retinal dystrophy that was proposed to reflect structural and functional defects in bipolar cells (as reflected by ERG b- and d-waves) (Henderson et al., 2009). *Otx2*$^{+/GFP}$ mice, therefore, may provide a useful model for understanding the visual impairments seen in *OTX2* mutant human patients. We use the mice to show that post-synaptic exogenous Otx2 protects OFF-type bipolar cells from glutamate excitotoxicity in the dark (Figure 7). Owing to inherent daily light cycle, the retinal dystrophies are unavoidable to *OTX2*-haplodeficient human and mice unless Otx2 is supplied externally. Therefore, intraocular Otx2 injection, which we found to attenuate visual loss in *Otx2*$^{+/GFP}$ mice, represents an intriguing potential therapeutic intervention for human patients.

EXPERIMENTAL PROCEDURES

Mice

The *Otx2*$^{+/GFP}$ mice, in which GFP is knocked into one allele of *Otx2*, were developed as previously reported (Di Salvio et al., 2010). The *Otx2*$^{fl/fl}$, *Crx-CreER*^{t2}, and *Chx10-CreER*^{t2} mice were generated as described in previous reports (Fossat et al., 2006; Muranishi et al., 2011). Experiments were carried out according to the guidance of the European Community Council directives of November 24, 1986 (86/609/EEC) and KAIST IACUC-12-110.

Multielectrode Array Recording of the Retina

Multielectrode array (MEA) recordings were obtained from flat-mounted retina isolated from P90 mouse eyes. The retinas were placed on a cellulose membrane and gently pressed against a multi-electrode array (MEA256 100/30 iR-ITO, Multichannel Systems, Germany) with RGCs facing to the electrodes. The retina was continuously superfused with Ames medium (Sigma-Aldrich) at 34°C at a rate of 1–2 ml/min, bubbled with 95% O_2 and 5% CO_2. Stock solution of metabotropic glutamate receptor (mGluR) agonist L-(+)-2-Amino-4-phosphonobutyric acid (L-AP4, Tocris Bioscience) was diluted to working concentrations of 50 μM and was bath-applied 10 min prior to recordings. Full-field light stimuli were applied to the samples for 2 s with 10-s interval by using a Polychrome V monochromator (Olympus) driven by a STG2008 stimulus generator (MCS) at 10^{14} photons × cm^{-2} × s^{-1}. Raw RGC activity recorded by MEA was amplified and sampled at 20 kHz. Resulting data were stored and filtered with a 200-Hz high-pass filter. Raster plots were obtained using threshold detection. Peristimulus time histogram (PSTH) was plotted in MATLAB. Single-cell PSTH was plotted on Spike2. Statistical analysis was done in GraphPad Prism v.6.

Histology and Cell Counting

Otx2$^{+/+}$ and *Otx2*$^{+/GFP}$ littermate mice were perfused with 4% paraformaldehyde (PFA) in PBS after anesthesia by tribromoethanol (Avertin). The eyes were then enucleated and fixed in 4% PFA and 20% isopropyl alcohol in sterile water for 2 days at room temperature for paraffin section or a serial incubation in 4% PFA/PBS and 25% sucrose/PBS for 16 hr at 4°C for frozen cryosection. Samples were embedded in paraffin and OCT medium for paraffin-embedded sections (5 μm) and cryosection (10 μm), respectively. Sections were stained with H&E for analyzing anatomical features of the retina. Images of retinal sections that included the optic head were acquired, and then a composite of the entire eye image was made using Nikon NIS software. After converting to gray scale, cells in different sections were counted manually and averaged.

(G) Mitochondrial transmembrane potential ($\Delta\Psi_m$) was examined by staining fresh frozen sections (30 μm) of P15 mouse retinas with TMRE (tetramethylrhodamine, ethyl ester) fluorescent dye (see details in Experimental Procedures). Dye trapped in the healthy mitochondria in the retinal sections was then visualized by confocal microscopy.

(H) Image pixels at the OPL areas of the sections were compared to obtain relative TMRE intensity values. Data were obtained by three different retinas for each group. *p < 0.05; ***p < 0.001.

Immunohistochemistry

Deparaffinized or dried frozen sections were rehydrated in PBS with 0.2% Tween 20 and permeabilized in PBS with 1% Triton X-100, 0.2% Tween 20, and 10% normal donkey serum. The sections were immunolabeled with corresponding primary antibodies, which were then visualized with the secondary antibodies conjugated with Alexa 488, Cy3, or Cy5. Nuclei of cells were visualized with 200 nM Hoescht 33342 (Hoe; Sigma), and fluorescent images were obtained using an Olympus Fluoview1000 confocal microscope. List of antibodies used for this study are provided in Table S2.

In Situ Hybridization

The full-length cDNA of mouse *Otx2* in pGEM-T vector were used to generate the sense and antisense RNA probes by T7 and SP6 RNA polymerases, respectively. In situ hybridization (ISH) was performed on cryosections with the digoxigenin (DIG)-labeled RNA probes. Hybridization was performed at 65°C for 18 hr followed by washes with 2 × saline sodium citrate (SSC) and 0.2 × SSC at 65°C. For detection of mRNA and proteins simultaneously, the sections were co-stained with primary antibodies detecting the marker proteins and alkaline phosphatase (AP)-conjugated anti-DIG Fab fragments (Roche) detecting the DIG-labeled probes. The anti-DIG Fab fragments bound to the DIG-labeled RNA probes were visualized by HNPP fluorescent detection set (Roche) after staining with fluorophore-labeled secondary antibodies detecting the primary antibodies. Fluorescent images of the ISH and IHC signals were then obtained by Olympus FV1000 confocal microscope.

Isolation of Mitochondria from Mouse Retinal Neurons

Mitochondria were isolated from retinal cells by stepwise centrifugation as described in a previous report (Heo et al., 2012). For detection of Otx2 at mitochondria, 25 μg of isolated mitochondria was resuspended in PBS or PBS with 0.5 M NaCl for the incubation in ice for 10 min. Alternatively, same amount of mitochondria were treated with PBS containing 100 ng/ml of proteinase-K at 37°C for 20 min. The mitochondria were then reprecipitated by centrifugation at 17,000 × *g* for 10 min for western blot (WB) analyses of supernatant and mitochondrial precipitates.

Mitochondrial ATP Synthesis Assay

ATP levels in the isolated mitochondria were measured with the ENLIGHTEN ATP assay system bioluminescence kit (Promega). In brief, purified mitochondria (50 μg/ml) were pre-incubated with Otx2-myc (0.5 μg/ml) for 30 min in ice before adding ADP (10 μM) and subsequent measuring ATP level in solution at specific time points. Chemiluminescence of samples was assessed with a MICROLUMAT LB96P Reader (Berthold). Three individual samples were assessed from each replicate to ensure internal consistency of the sample. The concentration of ATP was calculated from a standard curve (0.01–100 nM).

Mitochondrial Transmembrane Potential ($\Delta\Psi_m$) Detection in Retinal Sections

Mitochondrial transmembrane potential was measured by detecting the fluorescence emitted by Tetra methyl rhodamine ethyl ester (TMRE; Invitrogen) dye. The eyes removed of cornea and lens were incubated in DMEM with 50 nM TMRM for 45 min at 37°C in the dark and washed in 1 × HBSS before embedding in the OCT medium for freezing. Tissue slices were then prepared with a thickness of 30 μm by cryosection and fluorescent images of the retinas were obtained by Olympus FV1000 confocal microscope (excitation, 559 nm; emission range, 575–675 nm).

Statistical Analyses

Statistical analysis has been performed with SAS software (v.9.4). Group comparison was done using two-sample Student's t tests, unless otherwise specified in figure legends. A difference was considered significant at $p < 0.05$.

SUPPLEMENTAL INFORMATION

Supplemental Information includes Supplemental Experimental Procedures, seven figures, and two tables and can be found with this article online at http://dx.doi.org/10.1016/j.celrep.2015.09.075.

ACKNOWLEDGMENTS

We greatly appreciate Drs. Alain Prochiantz, Kenneth L. Moya, and Raoul Torero Ibad for supporting this work by sharing materials and resources. We also thank Drs. Edward Levin and Mi-Ryoung Song for generous gifts of Vsx1 and Vsx2 antibodies, respectively. This work was supported by the National Research Foundation of Korea (NRF) grants (NRF-2009-00424 (J.W.K.); NRF-2013M3C7A1056566 (J.W.K.); NRF-2014R1A2A2A01003069 (J.W.K.); NRF-2014K2A1C2074258 (J.W.K.); NRF-2013R1A1A2008459 (H.-T.K.); NRF-2012-R1A2A1A03002833 (M.S.) funded by the Korean Ministry of Science, ICT, and Future Planning (MSIP); and by funds from Korea Basic Science Institute (D34403 to J.S.C.; E35700 to H.-S.K.).

Received: September 1, 2015
Revised: September 15, 2015
Accepted: September 25, 2015
Published: October 22, 2015

REFERENCES

Acampora, D., Mazan, S., Lallemand, Y., Avantaggiato, V., Maury, M., Simeone, A., and Brûlet, P. (1995). Forebrain and midbrain regions are deleted in Otx2-/- mutants due to a defective anterior neuroectoderm specification during gastrulation. Development *121*, 3279–3290.

Alvarez-Fischer, D., Fuchs, J., Castagner, F., Stettler, O., Massiani-Beaudoin, O., Moya, K.L., Bouillot, C., Oertel, W.H., Lombès, A., Faigle, W., et al. (2011). Engrailed protects mouse midbrain dopaminergic neurons against mitochondrial complex I insults. Nat. Neurosci. *14*, 1260–1266.

Béby, F., Housset, M., Fossat, N., Le Greneur, C., Flamant, F., Godement, P., and Lamonerie, T. (2010). Otx2 gene deletion in adult mouse retina induces rapid RPE dystrophy and slow photoreceptor degeneration. PLoS ONE *5*, e11673.

Bernard, C., Kim, H.T., Torero Ibad, R., Lee, E.J., Simonutti, M., Picaud, S., Acampora, D., Simeone, A., Di Nardo, A.A., Prochiantz, A., et al. (2014). Graded Otx2 activities demonstrate dose-sensitive eye and retina phenotypes. Hum. Mol. Genet. *23*, 1742–1753.

Beurdeley, M., Spatazza, J., Lee, H.H., Sugiyama, S., Bernard, C., Di Nardo, A.A., Hensch, T.K., and Prochiantz, A. (2012). Otx2 binding to perineuronal nets persistently regulates plasticity in the mature visual cortex. J. Neurosci. *32*, 9429–9437.

Bovolenta, P., Mallamaci, A., Briata, P., Corte, G., and Boncinelli, E. (1997). Implication of OTX2 in pigment epithelium determination and neural retina differentiation. J. Neurosci. *17*, 4243–4252.

Chaban, Y., Boekema, E.J., and Dudkina, N.V. (2014). Structures of mitochondrial oxidative phosphorylation supercomplexes and mechanisms for their stabilisation. Biochim. Biophys. Acta *1837*, 418–426.

Derouiche, A., and Rauen, T. (1995). Coincidence of L-glutamate/L-aspartate transporter (GLAST) and glutamine synthetase (GS) immunoreactions in retinal glia: evidence for coupling of GLAST and GS in transmitter clearance. J. Neurosci. Res. *42*, 131–143.

DeVries, S.H., and Schwartz, E.A. (1999). Kainate receptors mediate synaptic transmission between cones and 'Off' bipolar cells in a mammalian retina. Nature *397*, 157–160.

Di Salvio, M., Di Giovannantonio, L.G., Acampora, D., Prosperi, R., Omodei, D., Prakash, N., Wurst, W., and Simeone, A. (2010). Otx2 controls neuron subtype identity in ventral tegmental area and antagonizes vulnerability to MPTP. Nat. Neurosci. *13*, 1481–1488.

Feng, L., Xie, X., Joshi, P.S., Yang, Z., Shibasaki, K., Chow, R.L., and Gan, L. (2006). Requirement for Bhlhb5 in the specification of amacrine and cone bipolar subtypes in mouse retina. Development *133*, 4815–4825.

Fossat, N., Chatelain, G., Brun, G., and Lamonerie, T. (2006). Temporal and spatial delineation of mouse Otx2 functions by conditional self-knockout. EMBO Rep. *7*, 824–830.

Henderson, R.H., Williamson, K.A., Kennedy, J.S., Webster, A.R., Holder, G.E., Robson, A.G., FitzPatrick, D.R., van Heyningen, V., and Moore, A.T. (2009). A rare de novo nonsense mutation in OTX2 causes early onset retinal dystrophy and pituitary dysfunction. Mol. Vis. *15*, 2442–2447.

Heo, J.Y., Park, J.H., Kim, S.J., Seo, K.S., Han, J.S., Lee, S.H., Kim, J.M., Park, J.I., Park, S.K., Lim, K., et al. (2012). DJ-1 null dopaminergic neuronal cells exhibit defects in mitochondrial function and structure: involvement of mitochondrial complex I assembly. PLoS ONE *7*, e32629.

Hide, T., Hatakeyama, J., Kimura-Yoshida, C., Tian, E., Takeda, N., Ushio, Y., Shiroishi, T., Aizawa, S., and Matsuo, I. (2002). Genetic modifiers of otocephalic phenotypes in Otx2 heterozygous mutant mice. Development *129*, 4347–4357.

Housset, M., Samuel, A., Ettaiche, M., Bemelmans, A., Béby, F., Billon, N., and Lamonerie, T. (2013). Loss of Otx2 in the adult retina disrupts retinal pigment epithelium function, causing photoreceptor degeneration. J. Neurosci. *33*, 9890–9904.

Kim, Y.H., Haidl, G., Schaefer, M., Egner, U., Mandal, A., and Herr, J.C. (2007). Compartmentalization of a unique ADP/ATP carrier protein SFEC (Sperm Flagellar Energy Carrier, AAC4) with glycolytic enzymes in the fibrous sheath of the human sperm flagellar principal piece. Dev. Biol. *302*, 463–476.

Koike, C., Nishida, A., Ueno, S., Saito, H., Sanuki, R., Sato, S., Furukawa, A., Aizawa, S., Matsuo, I., Suzuki, N., et al. (2007). Functional roles of Otx2 transcription factor in postnatal mouse retinal development. Mol. Cell. Biol. *27*, 8318–8329.

Martinez-Morales, J.R., Signore, M., Acampora, D., Simeone, A., and Bovolenta, P. (2001). Otx genes are required for tissue specification in the developing eye. Development *128*, 2019–2030.

Matsuo, I., Kuratani, S., Kimura, C., Takeda, N., and Aizawa, S. (1995). Mouse Otx2 functions in the formation and patterning of rostral head. Genes Dev. *9*, 2646–2658.

Mattson, M.P., Gleichmann, M., and Cheng, A. (2008). Mitochondria in neuroplasticity and neurological disorders. Neuron *60*, 748–766.

Miura, G., Wang, M.H., Ivers, K.M., and Frishman, L.J. (2009). Retinal pathway origins of the pattern ERG of the mouse. Exp. Eye Res. *89*, 49–62.

Muranishi, Y., Terada, K., Inoue, T., Katoh, K., Tsujii, T., Sanuki, R., Kurokawa, D., Aizawa, S., Tamaki, Y., and Furukawa, T. (2011). An essential role for RAX homeoprotein and NOTCH-HES signaling in Otx2 expression in embryonic retinal photoreceptor cell fate determination. J. Neurosci. *31*, 16792–16807.

Nieto, P.S., Valdez, D.J., Acosta-Rodríguez, V.A., and Guido, M.E. (2011). Expression of novel opsins and intrinsic light responses in the mammalian retinal ganglion cell line RGC-5. Presence of OPN5 in the rat retina. PLoS ONE *6*, e26417.

Nishida, A., Furukawa, A., Koike, C., Tano, Y., Aizawa, S., Matsuo, I., and Furukawa, T. (2003). Otx2 homeobox gene controls retinal photoreceptor cell fate and pineal gland development. Nat. Neurosci. *6*, 1255–1263.

Omori, Y., Katoh, K., Sato, S., Muranishi, Y., Chaya, T., Onishi, A., Minami, T., Fujikado, T., and Furukawa, T. (2011). Analysis of transcriptional regulatory pathways of photoreceptor genes by expression profiling of the Otx2-deficient retina. PLoS ONE *6*, e19685.

Ragge, N.K., Brown, A.G., Poloschek, C.M., Lorenz, B., Henderson, R.A., Clarke, M.P., Russell-Eggitt, I., Fielder, A., Gerrelli, D., Martinez-Barbera, J.P., et al. (2005). Heterozygous mutations of OTX2 cause severe ocular malformations. Am. J. Hum. Genet. *76*, 1008–1022.

Sato, S., Inoue, T., Terada, K., Matsuo, I., Aizawa, S., Tano, Y., Fujikado, T., and Furukawa, T. (2007). Dkk3-Cre BAC transgenic mouse line: a tool for highly efficient gene deletion in retinal progenitor cells. Genesis *45*, 502–507.

Sato, S., Omori, Y., Katoh, K., Kondo, M., Kanagawa, M., Miyata, K., Funabiki, K., Koyasu, T., Kajimura, N., Miyoshi, T., et al. (2008). Pikachurin, a dystroglycan ligand, is essential for photoreceptor ribbon synapse formation. Nat. Neurosci. *11*, 923–931.

Schröder, R. (2003). The genes orthodenticle and hunchback substitute for bicoid in the beetle Tribolium. Nature *422*, 621–625.

Schultz, B.E., and Chan, S.I. (2001). Structures and proton-pumping strategies of mitochondrial respiratory enzymes. Annu. Rev. Biophys. Biomol. Struct. *30*, 23–65.

Shiells, R.A., Falk, G., and Naghshineh, S. (1981). Action of glutamate and aspartate analogues on rod horizontal and bipolar cells. Nature *294*, 592–594.

Simeone, A., Puelles, E., and Acampora, D. (2002). The Otx family. Curr. Opin. Genet. Dev. *12*, 409–415.

Spatazza, J., Lee, H.H., Di Nardo, A.A., Tibaldi, L., Joliot, A., Hensch, T.K., and Prochiantz, A. (2013). Choroid-plexus-derived Otx2 homeoprotein constrains adult cortical plasticity. Cell Rep. *3*, 1815–1823.

Sugiyama, S., Di Nardo, A.A., Aizawa, S., Matsuo, I., Volovitch, M., Prochiantz, A., and Hensch, T.K. (2008). Experience-dependent transfer of Otx2 homeoprotein into the visual cortex activates postnatal plasticity. Cell *134*, 508–520.

Torero Ibad, R., Rheey, J., Mrejen, S., Forster, V., Picaud, S., Prochiantz, A., and Moya, K.L. (2011). Otx2 promotes the survival of damaged adult retinal ganglion cells and protects against excitotoxic loss of visual acuity in vivo. J. Neurosci. *31*, 5495–5503.

Vos, M., Lauwers, E., and Verstreken, P. (2010). Synaptic mitochondria in synaptic transmission and organization of vesicle pools in health and disease. Front. Synaptic Neurosci. *2*, 139.

Wieschaus, E., Nusslein-Volhard, C., and Kluding, H. (1984). Krüppel, a gene whose activity is required early in the zygotic genome for normal embryonic segmentation. Dev. Biol. *104*, 172–186.

Wyatt, A., Bakrania, P., Bunyan, D.J., Osborne, R.J., Crolla, J.A., Salt, A., Ayuso, C., Newbury-Ecob, R., Abou-Rayyah, Y., Collin, J.R., et al. (2008). Novel heterozygous OTX2 mutations and whole gene deletions in anophthalmia, microphthalmia and coloboma. Hum. Mutat. *29*, E278–E283.

Yoon, B.C., Jung, H., Dwivedy, A., O'Hare, C.M., Zivraj, K.H., and Holt, C.E. (2012). Local translation of extranuclear lamin B promotes axon maintenance. Cell *148*, 752–764.

Young, R.W. (1984). Cell death during differentiation of the retina in the mouse. J. Comp. Neurol. *229*, 362–373.

Young, R.W. (1985). Cell differentiation in the retina of the mouse. Anat. Rec. *212*, 199–205.